

Structure of bottle-brush brushes under good solvent conditions. A molecular dynamics study

Hamed Maleki¹ and Panagiotis E Theodorakis^{2,3,4}

¹ Institut für Physik, Johannes Gutenberg-Universität, Staudinger Weg 7, D-55099 Mainz, Germany

² Faculty of Physics, University of Vienna, Boltzmanngasse 5, A-1090 Vienna, Austria

³ Institute for Theoretical Physics and Center for Computational Materials Science, Vienna University of Technology, Hauptstraße 8-10, A-1040 Vienna, Austria

⁴ Vienna Computational Materials Laboratory, Sensengasse 8/12, A-1090 Vienna, Austria

E-mail: maleki@uni-mainz.de

E-mail: panagiotis.theodorakis@univie.ac.at

Abstract. We report a simulation study for bottle-brush polymers grafted on a rigid backbone. Using a standard coarse-grained bead-spring model extensive molecular dynamics simulations for such macromolecules under good solvent conditions are performed. We consider a broad range of parameters and present numerical results for the monomer density profile, density of the untethered ends of the grafted flexible backbones and the correlation function describing the range that neighboring grafted bottle-brushes are affected by the presence of the others due to the excluded volume interactions. The end beads of the flexible backbones of the grafted bottle-brushes do not access the region close to the rigid backbone due to the presence of the side chains of the grafted bottle-brush polymers, which stretch further the chains in the radial directions. Although a number of different correlation lengths exist as a result of the complex structure of these macromolecules, their properties can be tuned with high accuracy in good solvents. Moreover, qualitative differences with "typical" bottle-brushes are discussed. Our results provide a first approach to characterizing such complex macromolecules with a standard bead spring model.

PACS numbers: 02.70.Ns, 64.75.Jk, 82.35.Jk

Submitted to: *J. Phys.: Condens. Matter*

1. Introduction

Macromolecules with comb-like architecture, where linear or branched side chains are grafted onto a backbone chain have found much interest in recent years due to their physical and biochemical properties, which offer important benefits [1, 2, 3, 4, 5, 6, 7]. Although their structure is complicated, such macromolecules are being synthesized rather successfully [1, 2, 4, 8, 9]. Atom transfer radical polymerization has been efficiently applied to the synthesis of various bottle-brush brushes (also known as comb-on-comb brushes) [2, 4, 5, 10, 11], where bottle-brush molecules are grafted onto a linear chain (or a point (single monomer) in the case of star bottle-brush brushes) which serves as the backbone of the macromolecule. Brush polymers have been studied extensively as far as it concerns experiments [1, 2, 3, 4, 5, 6, 12, 13, 14] as well as theoretical modeling [15, 16, 17, 18, 19, 20, 21, 22, 23]. Already, the study of "typical" bottle-brush polymers (flexible linear polymeric chains grafted onto a backbone) has attracted attention for potential applications [1, 5]. For example, some work was motivated by the use of these cylindrical brushes as building blocks in functional supramolecular structures; applications for actuators and sensors have been also discussed, since the structure of these stimuli-responsive polymers can change when external parameters such as pH of the solution, temperature etc. are varied [24, 25]. The study of such effects has already been the subject of previous simulation studies of bottle-brush macromolecules with one or two types of side chains where a rigid backbone has been considered as a starting point for the study of these complex macromolecules [26, 27, 28, 29, 30, 31, 32, 33, 34, 35, 36], where it has also been shown that the radial density profiles for bottle-brush polymers with stiff and flexible backbones are similar when good solvent conditions are assumed. Bottle-brush brushes could serve as a candidate for applications already suggested for bottle-brush polymers, but in the case of bottle-brush brush polymers the higher number of varied structural parameters could help tuning the resulting properties of such macromolecules with a higher accuracy and in various ways. Also, towards understanding more complex structures of macromolecules which exist in biological systems, simulation models would allow for a better understanding of their complex structure-properties relation [37, 38].

Bottle-brush brushes exhibit rich structural behaviour providing even ideas for new applications due to the higher multitude of the correlation lengths which is expected from their structure. More interesting formations could be expected under poor solvent conditions as for typical bottle-brushes [26, 27, 28, 29, 30], but for bottle-brush brushes more difficulties, such as equilibrating such a systems, could be expected. Moreover, the interplay of the local conformation of side chains and the global configuration of the backbone adds more complexity to their intricate behaviour. The interpretation of experimental data on bottle-brush brushes is expected to be controversial as is already shown in the case of bottle-brushes with flexible linear side chains [32, 33]. Also, simulations has shown that the application of scaling concepts in the latter case is proven problematic even in the case where only a single type of side chains occurs, and

good solvent conditions are assumed [32, 33, 34, 35, 36]. Moreover, the application of theoretical arguments for the description of these macromolecules has been also proven very difficult [1, 3, 5, 6]. A comparison of the results of computer simulations could rather be realised on the basis of effective exponents, as for "typical" bottle brushes [31]. In view of the experimental interest for bottle-brush brushes and related complex macromolecules some fundamental understanding on their static properties can be achieved rather well by computer simulations. In this work we describe large-scale molecular dynamics simulations of an off-lattice model of a bottle-brush brush under good solvent conditions to provide a first approach to understanding their overall structural properties.

The outline of this paper is as follows. In Sec. 2 we describe the simulation model. Then, Section 3 discusses the analyzed properties and our numerical results, while Section 4 presents and summarizes our conclusions.

2. Computational details and simulation method

To simulate a bottle-brush brush polymer, we use a molecular dynamics method, where the monomers are coupled to a heat bath [39]. All the monomeric units are modeled by the standard bead-spring model [40, 41, 42, 43], where all monomers are treated as beads of mass m . This model has been extensively used in previous simulations of brush-like systems and its detail discussion has been given elsewhere [41]. Here, we give a brief description of the parameters we use in our simulations. For the interaction between any two monomers a truncated and shifted Lennard-Jones potential acts given by

$$U_{LJ}(r) = \begin{cases} 4\epsilon_{LJ}\left[\left(\frac{\sigma_{LJ}}{r}\right)^{12} - \left(\frac{\sigma_{LJ}}{r}\right)^6\right] + C & \text{for } r \leq r_c \\ 0 & \text{for } r > r_c \end{cases} \quad (1)$$

where $r_c = 2^{1/6}\sigma_{LJ}$ is the cut-off of the potential, and the constant C is defined such that $U_{LJ}(r = r_c)$ is continuous at the cut-off. Henceforth units are chosen such that $\epsilon_{LJ} = 1, \sigma_{LJ} = 1, k_B = 1$, and the mass m of the beads is also taken as unity. The connectivity of the beads is guaranteed by the "finitely extensible nonlinear elastic" (FENE) potential:

$$U_{FENE}(r) = -\frac{1}{2}kr_0^2 \ln\left[1 - \left(\frac{r}{r_0}\right)^2\right] \quad 0 < r \leq r_0, \quad (2)$$

where $r_0 = 1.5$, $k = 30$ and $U_{FENE}(r) = \infty$ outside the range written in equation (2). The equation of motion for each bead reads

$$m\frac{d^2\mathbf{r}_i}{dt^2} = -\nabla U_i - \gamma\frac{d\mathbf{r}}{dt} + \Gamma_i(t). \quad (3)$$

In this equation γ is the bead friction, $\Gamma_i(t)$ describes the random force of the heat bath and U_i is the potential each bead experiences due to the presence of the other beads, when they are below the cut-off distance. The random forces $\Gamma_i(t)$ satisfy the standard fluctuation-dissipation relation

$$\langle \Gamma_i(t) \cdot \Gamma_j(t') \rangle = 6k_B T \gamma \delta_{ij} \delta(t - t') \quad (4)$$

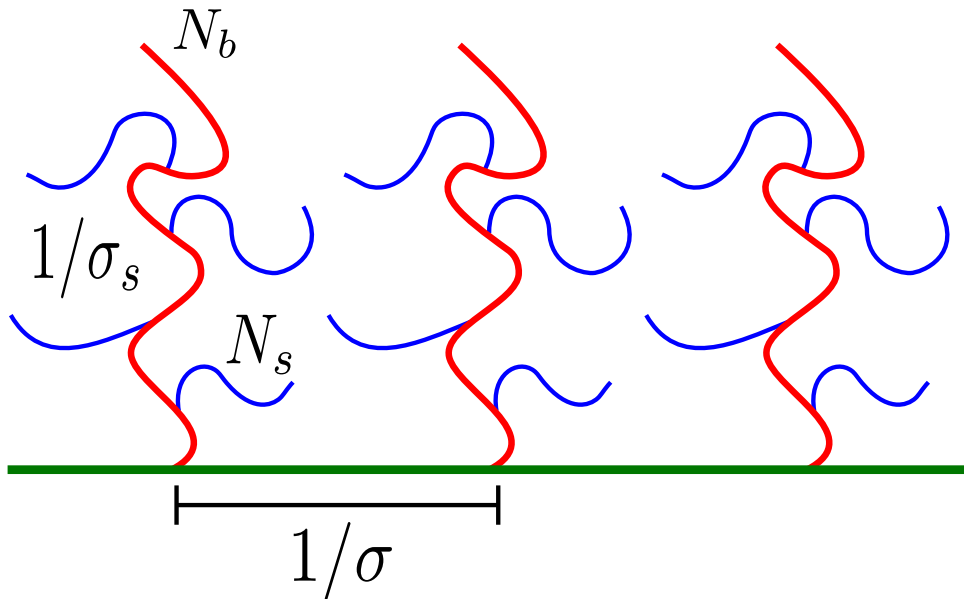


Figure 1: (Colour online) Schematic representation of bottle-brush brush polymer and parameters describing the structure of such system. σ is the grafted density that the bottle brush polymers are grafted onto the rigid backbone, N_b is the length of the flexible backbone. Also, flexible side chains of length N_s are grafted onto the flexible backbone with a grafting density σ_s .

where T is the temperature and k_B is the Boltzmann constant. Following previous work [39, 40, 41, 42, 43, 44, 45, 46] $\gamma = 0.5$ and $T = 1.2$. Here, $\tau = (m_{LJ}\sigma_{LJ}^2/\epsilon_{LJ})^{1/2}$ is the natural time unit, with units that have been given above. We use the the molecular dynamics package LAMMPS [47] to simulate our systems where the equations of motion for each bead (equation 3) are integrated with the velocity-Verlet scheme [48] with a time step $\Delta t = 0.008$. Periodic boundary conditions in the x -direction are applied, which is the axis of the rigid backbone where the brush chains with a flexible backbone are grafted regularly with a distance $1/\sigma$ between them. In this study we have considered different grafting densities, i.e., $\sigma = 0.25, 0.50$, and 1.00 , which corresponds to grafting every bead, every second bead, and every forth bead of the rigid backbone. Smaller densities for our range of chain lengths would suppress any effects due to the density, while higher grafting densities than the ones we consider here would impose difficulties in equilibrating our systems. In y - and z -directions, periodic boundary conditions are applied as well, but the considered linear dimensions of the simulation box were chosen large enough, so that never any interaction of the grafted bottle brush polymers with their periodic images could occur. We have considered a variety of parameters as they are schematically described in figure 1. The backbone where the chains are grafted with a grafting density σ is rigid, while the backbones of the grafted brushes onto this rigid backbone are flexible as well as their side chains. The number of monomers of the rigid backbone was $N = 128$. We have also performed simulations for other choices

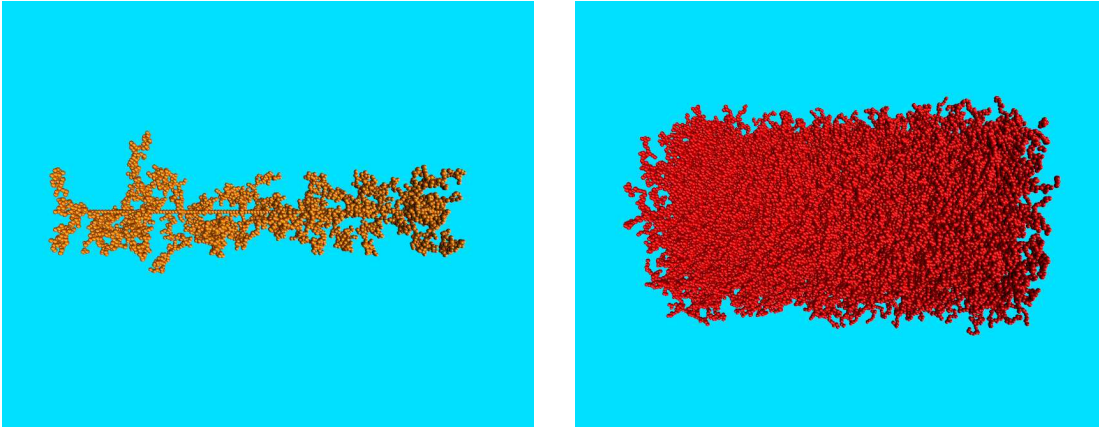


Figure 2: (Colour online) Two characteristic snapshots of bottle-brush brush polymers with different set of parameters. These snapshots show the different structures of bottle-brush brush polymers under good solvent conditions. This is similar to the behaviour of typical bottle-brush polymers. In the left snapshot the set of parameters $\sigma = 0.25$, $N_b = 12$, $N_s = 3$ and $\sigma_s = 0.50$ was chosen and for the right snapshot, $\sigma = 1.00$, $N_b = 48$, $N_s = 24$, $\sigma_s = 1.00$. Our choice of parameters show the different structures that may result ranging from low densed brushes to homogeneous cylinders.

of backbone lengths in order to check the influence of periodic boundary conditions on the resulting properties. We found that our results are not affected by the presence of periodic boundary conditions for the rigid backbone length that is taken here. However, if one tries to simulate such a system under poor solvent conditions, then one would expect an influence of the periodic boundary conditions on the properties of the grafted brushes [26, 27, 28, 29, 30]. In this manuscript, we will present only results for $N = 128$. The backbone of the bottle-brushes attached onto the rigid backbone is $N_b = 12, 24, 36$, and 48 (the part of the chains denoted with red color in figure 1). Higher lengths are prohibitely difficult to study. Also, it would be difficult for experiments to access such lengths as it has been discussed already for typical brushes [32]. For the side chains of the grafted bottle-brushes onto the rigid backbone we have typically considered chain lengths shorter than N_b , i.e., $N_s = 3, 6, 12$, and 24. These shorter side chains (denoted with blue color in figure 1) are grafted onto the flexible backbone of the brushes with a grafting density $\sigma_s = 0.5$ or 1.0. As shorter chain lengths are used for N_s , we did not study the grafting density $\sigma_s = 0.25$. Figure 2 shows (left part) typical snapshots for the case of $\sigma = 0.25$, $N_b = 48$, $N_s = 3$ and $\sigma_s = 0.5$. In the right part the case of $\sigma = 1.00$, $N_b = 48$, $N_s = 24$ and $\sigma_s = 0.5$ is shown. For our choice of parameters we observe structures ranging from low densed brushes to homogeneous cylinders.

We note here that equilibration of our systems required running our simulations for every brush for a time range of 20×10^6 MD time-steps. Then we collect 2000 samples running the simulations 4×10^6 MD steps further. By studying correlations functions for the structural properties of the brushes that vary slowly with time, we find out that

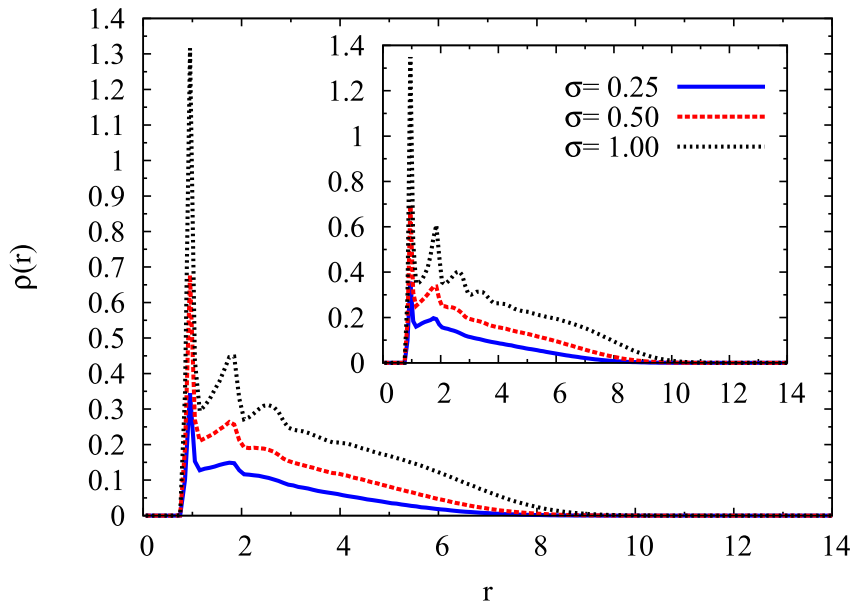


Figure 3: (Colour online) Density profile $\rho(r)$ as a function of r perpendicular to the rigid backbone for bottle-brush brush polymers with $N_b = 12$, $N_s = 3$ and $\sigma_s = 0.5$, for the grafting densities $\sigma = 0.25, 0.5$ and 1.0 . r is the distance from the rigid backbone. Inset shows results for the same set of parameters, but $\sigma_s = 1.0$

this effort was enough to obtain reliable results. In the following, we present our results discussing overall structural properties for these complex macromolecules providing an insight for the overall behavior of these polymers.

3. Results and Discussion

First, we focus on the effect of the grafting density σ on the density profile in the radial directions ($y - z$ plane with the rigid backbone extending along the x direction) for moderate values of N_b and N_s . Figure 3 shows the density profiles of the system in radial directions (y, z) for the case $N_b = 12$, $N_s = 3$ and different grafted densities σ . From figure 3, the increase of the grafting density σ shows that the chains overall become more stretched in the radial direction as it normally happens for typical bottle-brushes. For low grafting density σ , the density curves decay almost exponentially for $\sigma = 0.25$ and their height reflects analogously the corresponding grafting densities (the second peak from the left). Also, by increasing the grafting density σ the latter extension in density becomes higher as the side chains of the grafted brushes get stiffened due to the excluded volume interactions. Moreover, for $\sigma = 1.0$, figure 3 shows that the density profile persists over longer distances from the rigid backbone and indicates that the side chains of the grafted bottle-brush molecules tend to stretch in the radial directions. In addition, the increase of number of side chains grafted onto the flexible backbone σ_s (inset) hint the effect that the curves of density profile extend further, but the overall

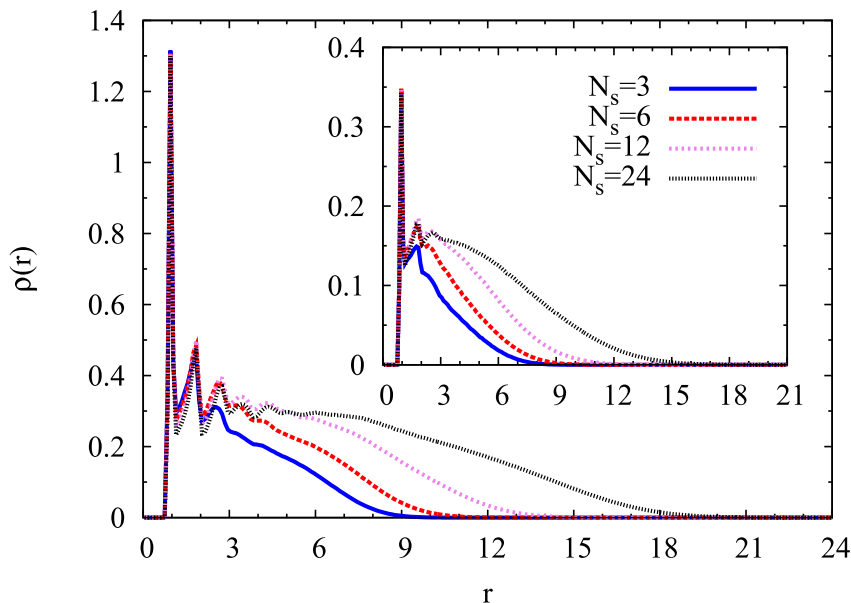


Figure 4: (Colour online) Variation of the density profile $\rho(r)$ as a function of r for the case of $\sigma = 1.00$, $N_b = 12$ and four different values of N_s ($\sigma_s = 0.5$). Inset shows the corresponding results for $\sigma = 0.25$.

behaviour of the systems does not change. Also, for the case $\sigma = 1$ and $\sigma_s = 1$ a third peak is formed due to the layering effect as the density increases close to the rigid backbone.

Stretching of the flexible grafted bottle-brushes in the radial directions is more pronounced when one changes the length of the side chains of the grafted bottle-brushes. Figure 4 shows differences in the density profile which result from the variation of N_s . The increase of N_s strengthens the extension of the density profile in the radial direction. The density now stays almost constant at rather high distances r (the density remains constant even at longer distances from the rigid backbone) and the resulting formation of the bottle-brush brush resembles a homogeneous cylinder as it is that of figure 2 (right part). For $\sigma = 1$ we see this rather constant density up to a distance 7 from the rigid backbone (disregarding of course the first two peaks, which are reminiscent of the layering effect observed for fluid particles in a box close to the wall). As N_s increases, the density profile extends to higher distances from the rigid backbone. This extension becomes a rather small effect as the grafting density σ is low enough that the beads can not fill the space close to the rigid backbone under good solvent conditions where the chains stretch in the radial direction (inset).

The variation of the density profile as a function of the radial distance r with N_b is shown in figure 5 (a). This typical graph is for the case of grafting density $\sigma = 0.25$ and $N_s = 24$. This "low" grafting density allows us to discuss the particular effects avoiding the structures where the density close to the rigid backbone is high. At small distances r from the rigid backbone, the difference in the density profiles can not be

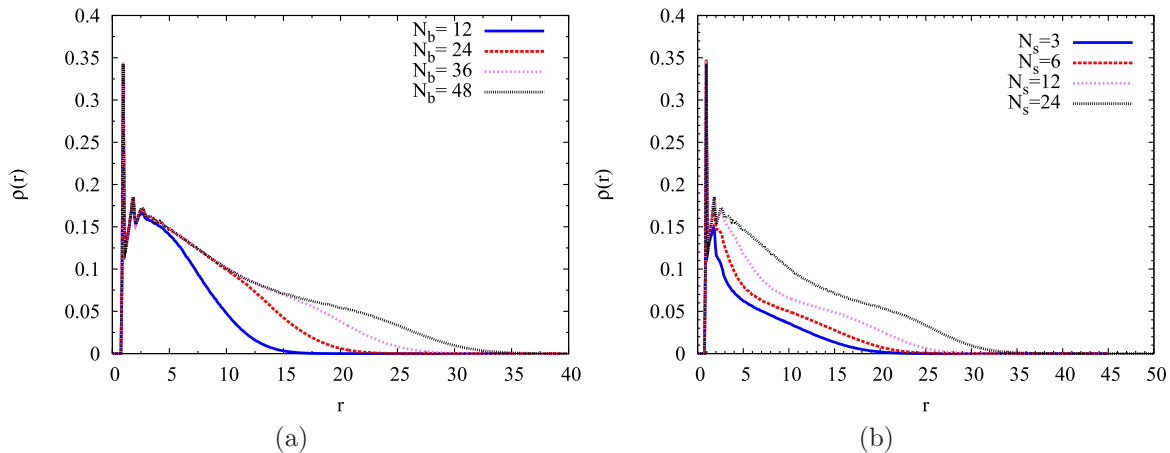


Figure 5: (Colour online) Density profile $\rho(r)$ plotted versus the radial distance r . (a) The case $\sigma = 0.25$, $N_s = 24$ and four different brush chain lengths N_b is shown. (b) Same as figure 4, for the case $\sigma = 0.25$, $N_b = 48$ and different values of N_s . $\sigma_s = 0.5$ in both cases (a) and (b).

seen. However, at higher distances, the effect of long side chains ($N_s = 24$) shows higher density at larger distances r . For $N_b < 24$ the density profile looks as it is rather expected even for a typical bottle-brush polymer. But for $N_b > 24$ (and $N_s = 24$) the density profile shows a completely different behaviour when the length of the side chains (N_s) is also rather high. This behavior is characteristic for the bottle-brush brush polymers. The density far from the rigid backbone is higher compared to a typical bottle-brush polymer. Without the side chains of the flexible brush, we would have expected and almost exponential decay in the density profile. However, as the length N_s increases (figure 4), the density in the outer region (far from the rigid backbone) of the bottle-brush brush polymer increases, and this difference is more pronounced, when the length N_b is high enough in order to be far from the almost constant density region close to the rigid backbone (figure 5 (b)).

More interesting is to study the behaviour of the ungrafted end beads of the bottle-brushes which are grafted on the rigid backbone in order to check how close they can come to the rigid backbone. Figure 6 shows our results for the distribution of these end beads and the dependence with grafting density σ . Since σ increases the peak of $\rho_E(r)$ becomes sharper and thinner. This indicates that the end beads of the flexible backbone are moving within a narrower space in the radial direction and they rather never reach the region close to the rigid backbone. This effect clearly shows that the chains are stiffened due to the increase of the grafting density σ and as a consequence, the peak is higher in the case of high σ . The stretching of the brush chains in the radial direction is also seen here and corroborates the results of figure 3. According to figure 6, as σ increases, the peaks are positioned at higher distances r . This effect is similar to the case of typical bottle-brush polymers where the increase of the grafting density

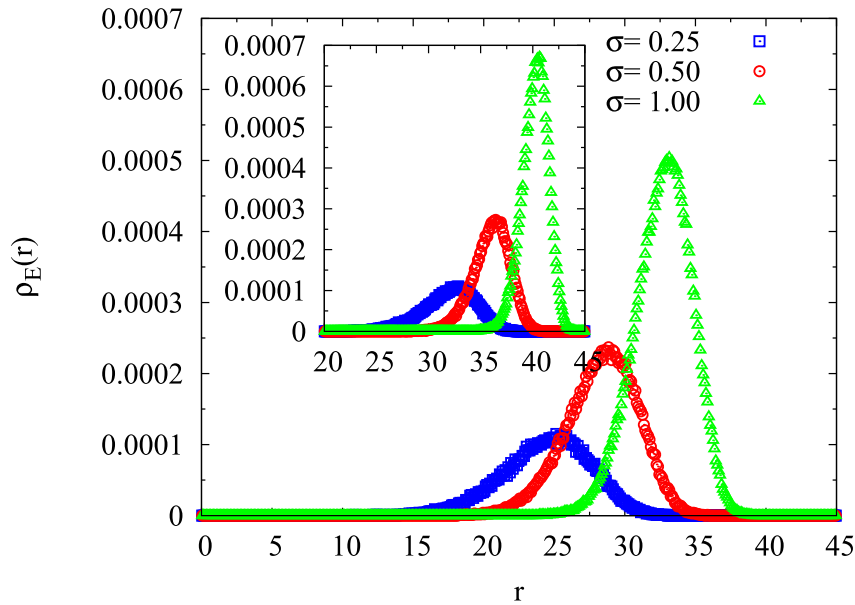


Figure 6: (Colour online) Density profiles of the untethered end beads of the flexible backbones (bottle brush chains) $\rho_E(r)$ as a function of radial distance r from the rigid backbone for different values of σ . This typical illustration is for a system with $N_b = 48$, $N_s = 24$ and $\sigma_s = 0.5$ ($\sigma_s = 1.0$ in inset).

induces stretching of the side chains in the radial directions and resulting in the increase of the zone which is not accessible to the end beads. The increase of σ_s strengthens the aforementioned effects, i.e., the brush chains become more stiffened and more stretched, although the chains are under very good solvent conditions.

The corresponding results for the end beads distribution for figure 5, i.e., figure 7, shows that the increase of N_b shifts the peaks of the resulting density profiles to the right, while these peaks become less sharp, lower and smoother, showing that the flexible backbone becomes less mobile in the radial directions even for this case where the length of the side chains of the brush N_s is rather high. Looking at figures 6 and 7, we can see that all the changes of parameters have a rather proportional effect on the properties. This points out that careful tuning of the structure of the bottle-brush brushes can result from the design of our macromolecules, which can be performed in a variety of ways, due to the variety of the parameters that describe their structure.

When σ_s increases, the differences in the curves are higher and one can see that the curves of the density profiles corresponding to different N_b do not overlap any more. The latter effect points us out that the increase of the grafting density σ_s has a significant effect and it is related analogously to the probability for the flexible backbone untethered end of coming close to the rigid backbone. Figure 8 confirms this conclusion. When $\sigma_s = 0.5$, for different values of N_s , we can almost observe the same height of the peaks in the density profiles for the end beads, the curves become slightly narrower, but the differences are not as pronounced as in the case of $\sigma_s = 1.00$. This clearly shows that

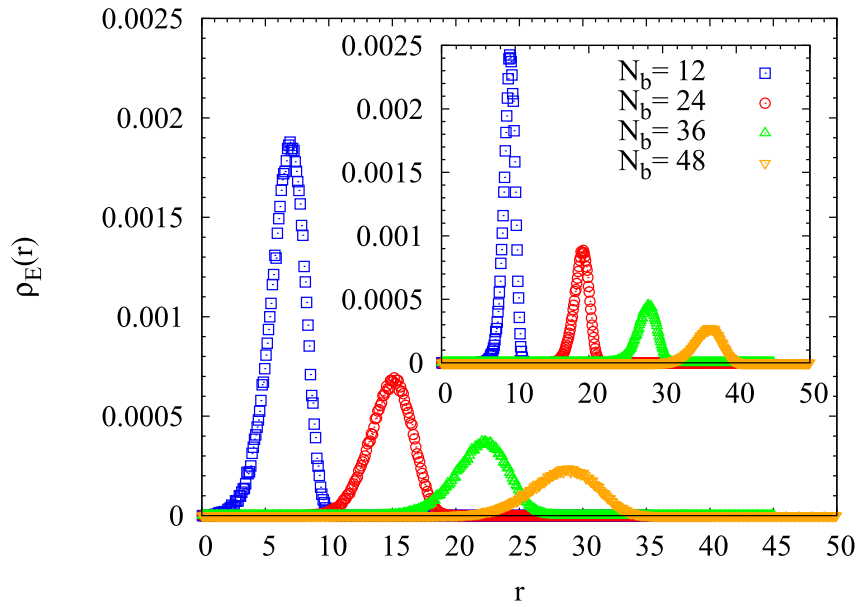


Figure 7: (Colour online) Same as figure 6, variation of density profile of the untethered end beads versus radial distance r for the case $\sigma = 0.50$, $N_s = 24$, and $\sigma_s = 0.5$ ($\sigma_s = 1.0$ as inset), and different values of N_b .

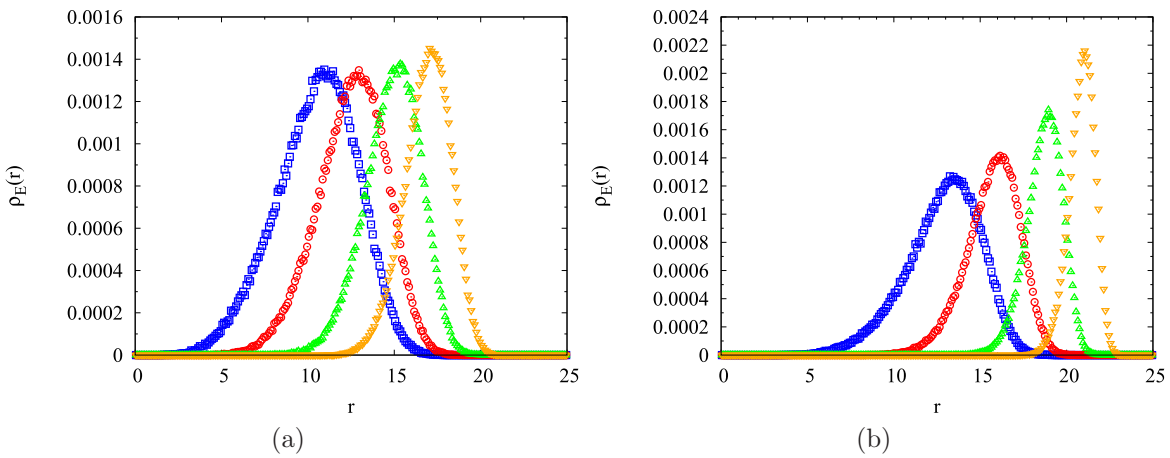


Figure 8: (Colour online) (a) Same as figure 6, the flexible backbone (brush chains) ends $\rho_E(r)$ vs. r for $\sigma = 1.00$, $N_b = 48$, and $\sigma_s = 0.5$ (b) $\sigma_s = 1.0$), and different values of $N_s = 3(\square)$, $6(\circ)$, $12(\triangle)$ and $24(\nabla)$.

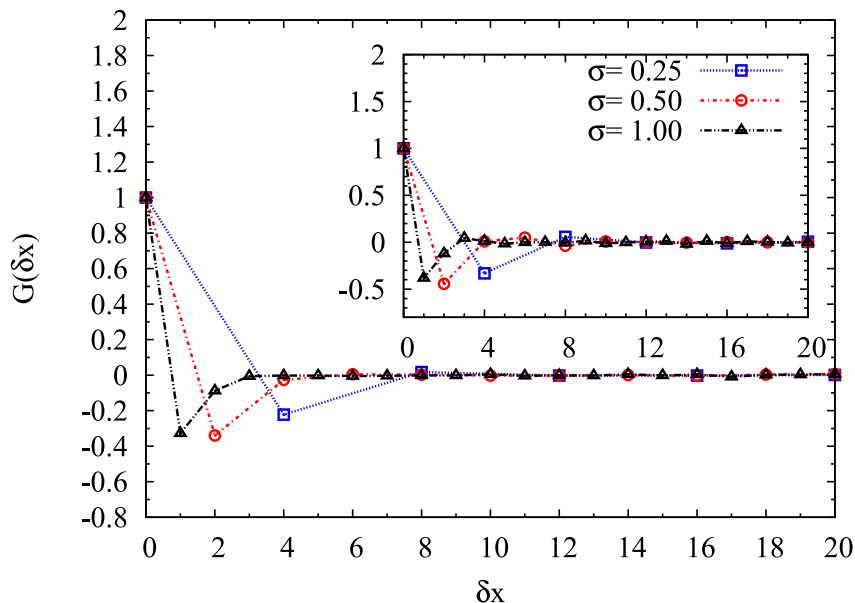


Figure 9: (Colour online) The orientation correlation function $G(\delta x)$ as a function of the correlation distance δx along the rigid backbone for a bottle-brush brush polymer with parameters $N_b = 12$, $N_s = 3$ and $\sigma_s = 0.5$ ($\sigma_s = 1.0$ in inset) for different grafting density σ . Only a range of δx is shown.

the change in the grafting density σ_s has a significant effect on the bottle-brush brush polymers, which we could not distinguish in the overall radial density profiles. We should also note that the increase of σ_s introduces noticeable differences in the height of the peaks, showing that this parameter can play an important role in the resulting behaviour of our system showing that the variations in N_s result in more pronounced differences in the peaks for high grafting density of side chains ($\sigma_s = 1.0$), and they now have a better correspondence to the values of N_s .

Figures 9 and 10 show the correlation functions of orientations of different bottle-brushes in order to monitor the extent over which correlations between the different grafted brushes on the rigid backbone persist [27]. Such a property has been mainly considered for bottlebrush polymers with two types of monomers [27] in order to characterize the extent over which a Janus structure exists. However, in our case it would provide us with information of the extent that these compact objects (bottle-brushes grafted on the rigid backbone at high densities) are affected by the presence of their neighboring bottle-brushes. For each chain the vector pointing from the grafting site (the monomer on the rigid backbone where the brush is grafted) to the center of mass of the respective grafted bottle-brush is considered. Projecting this vector into the yz -plane and defining a unit vector \vec{S}_i for the i -th bottle-brush, we define the correlation function

$$G(\delta x) = \langle \vec{S}_i \cdot \vec{S}_j \rangle. \quad (5)$$

As we can see from figure 9, the influence of the grafting density σ for values 0.25-1.00

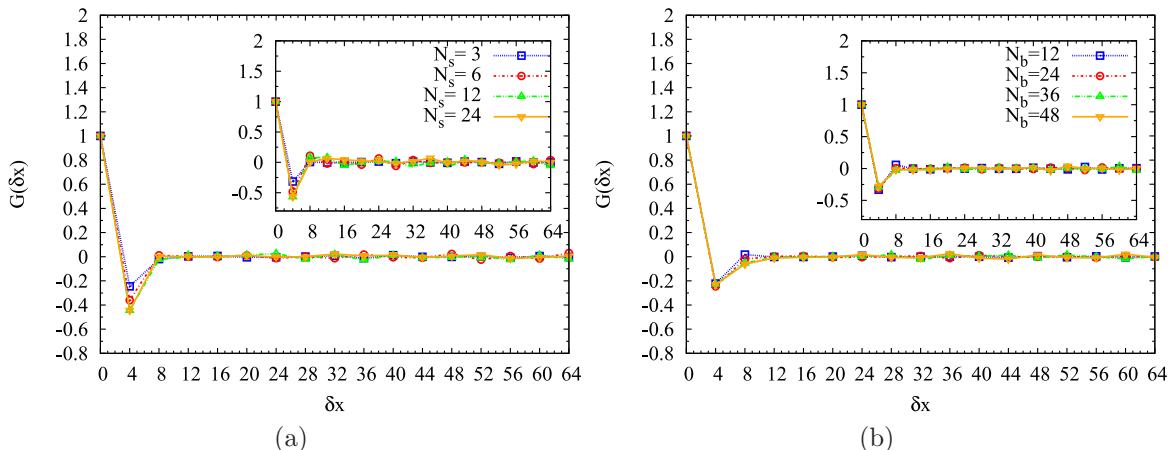


Figure 10: (Colour online) (a) The correlation function $G(\delta x)$ as a function of the distance δx along the rigid backbone for a bottle-brush brush polymer with fixed grafted density $\sigma = 0.25$, $N_b = 24$ and $\sigma_s = 0.5$ for different side chain length N_s (inset, $\sigma_s = 1.0$). (b) $G(\delta x)$ as a function of δx for a bottle-brush brush polymer with fixed grafted density $\sigma = 0.25$, $N_s = 3$ and $\sigma_s = 0.5$ with different chain lengths N_b (inset, $\sigma_s = 1.0$). The first peak is at $1/\sigma$.

is small, and only some difference can be observed when the value of σ changes from 0.25 to 0.50. Further increase of the grafting density σ seems to have a small effect on the chains. These conclusions are also confirmed for other set of parameter N_b and N_s (not shown here). We should emphasize that these first peaks occur at a distance $1/\sigma$ as expected. Furthermore, the same behaviour is observed when the grafting density σ_s is increased (inset in figure 9). What we see is that the neighbour bottle-brushes influence mainly their first neighbours. Two neighbouring brushes grafted on the rigid backbone tend to orient in different directions due to the excluded volume interactions, whereas the second neighbours, the third, etc., are almost unaffected from the presence of the other grafted bottle-brushes on the rigid backbone. Only in the case that $\sigma = 1.00$ some correlation is slightly detected also for the second neighbors. Deviations for $G(\delta x)$ from zero for third, fourth, fifth, etc. neighboring grafted brushes (figure 9) are within the statistical error. Of course, this is due to the short chain lengths we have considered for our flexible brushes. When the radius of gyration of the grafted brushes would be higher, these effects play more important role.

For the set of parameters of figure 10, we have varied parameters N_b and N_s . Here we show only results for the case $\sigma = 0.25$, in order to discuss the particular effects. Similar conclusions are drawn for the other cases. Also the increase of N_s (figure 10(a)) shows that the correlations increase, but for $N_s > 6$ the occurring differences are smaller. The variation of N_b (figure 10 (b)) leads to the same conclusion. For the results of figures 9 and 10, we can further observe that the increase of σ_s results in the increase of the correlations (which of course takes a negative value for neighboring brushes) along the

rigid backbone, as the density of the monomers increases. The increase of σ_s from 0.50 to 1.00 increases significantly the density of the monomers between the backbone of the grafted bottle-brushes, effect which is seen in the results of this correlation function. But even in the case of long lengths N_s and N_b and high grafting densities grafted bottle-brushes further apart from the first neighbors are hardly influenced. To conclude, for the the small lengths N_b and N_s considered here, the main effect comes from the variation of the grafting density. For other combinations of parameters (not shown here in order to save space) the conclusions remain the same.

4. Summary

In the present study, we performed molecular dynamic simulations of a standard bead-spring model of flexible bottle-brush polymers grafted onto a rigid backbone under good solvent conditions. Our investigation was based on the analysis of overall properties of interest, i.e., the density profiles in the radial directions (which is the perpendicular direction to the rigid backbone where the bottle-brush polymers are grafted with one of the ends of their flexible backbone). We discussed that the increase of any of the parameters σ , σ_s , N_b , and N_s results in the stretching of the bottle-brushes in the radial directions although we are under good solvent conditions, as has been also discussed for typical bottle-brushes with a rigid or a flexible backbone. We can also clearly see by analysis of the correlation function $G(\delta x)$ that mainly only first neighbor grafted bottle-brush chains are affected due to the excluded volume interactions between their monomers, even for our extreme cases where the grafted densities σ and σ_s , and the lengths N_b and N_s are high. As the size of the grafted brushes increases, this effect is expected to be more pronounced. The strength of the excluded volume effects between two neighboring bottle-brush polymers grafted onto the rigid backbone can be tuned in various ways, due to the high number of structural parameters characterizing such macromolecules, compared to a typical bottle-brush polymer under good solvent conditions, where the only varying parameter (considering also a rigid backbone) is the length of the grafted linear polymeric chains and the grafting density σ . We found that the variation of these parameters affect in a proportional way the properties of the macromolecules. That is a change of one parameter for all the grafted brushes has an analogous measurable effect to the structural properties of these macromolecules, although at a first glance their structure seems complicated to be studied by computer simulations. Thus, the properties of these macromolecules can be tuned efficiently by the change of parameters, of course when these are in a good solvent. The lengths of the chains in our study were rather short, but we should stress here that such lengths could be also accessible in the synthesis of bottle-brush brushes. We also find that for the range of parameters studied here, the untethered ends of the chains have not any possibility of being anywhere close to the rigid backbone even for small σ . The distance and the range that these end beads (possible carriers of some particular substance) can access close to the backbone can also efficiently be tuned, which is rather impossible

to control with such accuracy in a typical bottle-brush with flexible side chains. The width of this zone (unaccessible to the end beads) depends strongly on the N_s and σ_s and on the increase of the density depending on the other parameters. We hope that our results will stimulate further study of these macromolecules and the work of analytical predictions.

Acknowledgment

Authors are grateful to Zentrum für Datenverarbeitung (ZDV) in uni-mainz for the computer facilities. P.E.T. is grateful for financial support by the Austrian Science Foundation within the SFB ViCoM (grant F41).

References

- [1] Zhang M and Müller A H E 2005 *J. Polym. Sci. Part A: Polym. Chem.* **43** 3461
- [2] Koutalas G, Iatrou H, Lohse D and N. Hadjichristidis 2005 *Macromolecules* **38** 4996
- [3] Subbotin A V and Semenov A N 2007 *Polymer Science, Ser. A* **49** 1328
- [4] Ishizu K, Murakami T and Takano T 2008 *J. colloid and interface sci.* **322** 59
- [5] Sheiko S S, Sumerlin B S and Matyjaszewski K 2008 *Progr. Polym. Sci.* **33** 759
- [6] Potemkin I I and Palyulin V V 2009 *Polymer Science, Ser. A* **51** 163
- [7] Schappacher M and Deffieux A 2000 *Macromolecules* **33** 7371
- [8] Wintermatnel M, Gerle M, Fischer K, Schmidt M, Wataoka I, Urakawa H, Kajiwara K and Tsukahara Y 1996 *Macromolecules* **29**, 978
- [9] Gunari N, Cong Y, Zhang B, Janshoff A and Schmidt M 2008 *Macromol. Rapid Commun.* **29** 821
- [10] Matyjaszewski K and Xia J 2001 *Chem. Rev.* **101** 2921
- [11] Matyjaszewski K, Qin S, Boyce J R, Shirvanyants D and Sheiko S S 2003 *Macromolecules* **36** 1843
- [12] Rathgeber S, Pakula T, Matyjaszewski K and Beers K L 2005 *J. Chem. Phys.* **122** 124904
- [13] Zhang B, Gröhn F, Pedersen J S, Fischer K, Schmidt M 2006 *Macromolecules* **39** 8440
- [14] Rathgeber S, Pakula T, Wilk A, Matyjaszewski K, Lee H -I and Beers K L 2006 *Polymer* **47** 7318
- [15] Alexander S 1977 *J. Phys.(Paris)* **38** 983
- [16] de Gennes P -G 1980 *Macromolecules* **13** 1069
- [17] Daoud M and Cotton J 1982 *J. Phys.(Paris)* **43** 531
- [18] Bug A L R, Cates M E, Safran S A, and Witten T A 1987 *J. Chem. Phys.* **87** 1824
- [19] Milner S T, Witten T A and Cates M E 1988 *Europhys. Lett.* **5** 413
- [20] Milner S T, Witten T A and Cates M E 1988 *Macromolecules* **21** 2610
- [21] Milner S T 1991 *Science* **251** 905
- [22] Fredrickson G H 1993 *Macromolecules* **26** 2825
- [23] Zhulina E B and Vilgis T A 1995 *Macromolecules* **28** 1008
- [24] Stephan T, Muth S and Schmidt M 2002 *Macromolecules* **35** 9857
- [25] Li C, Gunari N, Fischer K, Janshoff A and Schmidt M 2004 *Angew. Chem. Int. Ed.* **43** 1101
- [26] Theodorakis P E, Paul W, and Binder K 2009 *Europhys. Lett.* **88** 63002
- [27] Theodorakis P E, Paul W and Binder K 2010 *Macromolecules* **43** 5137.
- [28] Theodorakis P E, Paul W and Binder K 2010 *J. Chem. Phys.* **133** 104901
- [29] Erukhimovich I, Theodorakis P E, Paul W and Binder K 2011 *J. Chem. Phys.* **134** 054906
- [30] Theodorakis P E, Paul W and Binder K 2010 *Eur. Phys. J. E* **34** 52
- [31] Theodorakis P E, Hsu H-P, Paul W and Binder K 2011 *J. Chem. Phys.*
- [32] Hsu H -P, Paul W, Rathgeber S and Binder K 2010 *Macromolecules* **43** 1592
- [33] Hsu H -P, Paul W and Binder K 2007 *Macromol. Theory Simul.* **16** 660
- [34] Hsu H -P, Paul W and Binder K 2008 *J. Chem. Phys.* **129** 204904

- [35] Hsu H -P, Paul W and Binder K 2006 *Europhys. Lett.* **76** 526
- [36] Hsu H -P, Binder K and Paul P 2009 *Phys. Rev. Lett.* **103** 198301
- [37] Klein J 2009 *Science* **323** 47
- [38] Chang R, Kwak Y and Gebremichael Y J 2009 *Mol. Biol.* **391** 648
- [39] Grest G S and Kremer K 1986 *Phys. Rev. A* **33** 3628
- [40] Graessley W W, Hayward R C and Grest G S *Macromolecules* **32** 3510
- [41] Grest G S and Murat M 1995 in *Monte Carlo and Molecular Dynamics Simulations in Polymer Science* Binder K Ed. p. 476. Oxford Univ. Press New York
- [42] Grest G S and Murat M 1993 *Macromolecules* **26** 3108
- [43] Murat M and Grest G S 1991 *Macromolecules* **27** 704
- [44] Grest G S 1999 *Adv. Polym. Sci.* **138** 149
- [45] Murat M and Grest G S 1989 *Macromolecules* **22** 4054
- [46] Grest G S 1994 *Macromolecules* **27** 418
- [47] <http://lammmps.sandia.gov/>
- [48] Plimpton S 1995 *J. Comput. Phys.* **117** 1